Environmental Science and Pollution Research (2022) 29:43984–44002
https://doi.org/10.1007/s11356-022-18760-8

RESEARCH ARTICLE

Analysis of degradation and pathways of three common antihistamine drugs by NaClO, UV, and UV-NaClO methods

Anchen Liu[1] · Wenting Lin[1] · Senwen Ping[1] · Wenqi Guan[1] · Ningyi Hu[1] · Sichun Zheng[1] · Yuan Ren[1,2,3]

Received: 21 October 2021 / Accepted: 15 January 2022 / Published online: 5 February 2022

Abstract

Antihistamines (ANTs) are medicines to treat allergic diseases. They have been frequently detected in the natural water environment, posing potential threats to the ecological environment and human health. In this study, the degradation of three common antihistamines, loratadine, fexofenadine, and cetirizine, was estimated under different oxidation methods (NaClO, UV, and UV-NaClO). The results showed that UV-NaClO had the highest degree of degradation on the drugs under most conditions: 100% degradation for fexofenadine within 20 s at pH 7 and 10. Under UV irradiation, the degradation efficiencies of the three drugs during 150 s were all above 77% at a pH of 7. The drugs' removal by NaClO was much lower than that of the previous two methods. In addition, this study explored the contribution rates of active oxygen species in the photolysis process. Among them, the contribution of $^1O_2$ to the fexofenadine and cetirizine removal rate reached 70%. Different aqueous matrices (HCO_3^-, NO_3^-, and humic acid) had varying degrees of influence on the degradation. Acute toxicity tests and ultraviolet scans of the degradation products showed that the drugs were not completely mineralized, and the toxicities of the intermediates were even higher than those of the parent drugs. There were 9, 8, and 10 chloride oxidation products of loratadine, fexofenadine, and cetirizine, respectively, and 8 photolysis products of cetirizine were identified. For cetirizine, it was found that there were three identical intermediates produced by photodegradation and NaClO oxidation.

Keywords Antihistamines · Sodium hypochlorite · UV irradiation · Aqueous matrix · Pathways · Acute toxicity

Introduction

Antihistamines have been widely used to treat a variety of diseases since they entered the market in the 1940s (Kristofco and Brooks 2017). Given the variety of uses, antihistamines have become the largest amount of drugs used to treat allergic diseases. According to the World Allergy Organization (WAO), the incidences of allergic asthma, rhinitis, urticarial, and pruritus have increased threefold, with a prevalence of 22% in the past 30 years. Antihistamines were included in the recommended drugs for first-line diagnosis and treatment (Zhang et al. 2021). These medicines have been developed through three generations. The use of the first-generation antihistamines, such as diphenhydramine and decloxizine, has decreased because of severe adverse effects. Second-generation antihistamines include loratadine (LOR), cetirizine (CER), and azelastine (Wu 2012); and third-generation antihistamines include fexofenadine (FEX) and levocetirizine. In China, the average annual production of LOR, FEX, and CER during 2015–2017 was 1.9, 0.79, and 40.6 tons, respectively (Editorial Department of Annual Report 2015, 2016, 2017).

All these drugs were discharged into wastewater treatment plants (WWTPs) in the form of the parent compounds or their metabolites after being taken by humans (Zhou et al. 2016). FEX and CER were excreted as the parent compounds; as a metabolite of LOR, desloratadine

Responsible Editor: Sami Rtimi

Highlights
1. UV-NaClO has the most efficent photodegradability than UV or NaClO alone.
2. $^1O_2$ played an important role in the process of drug photolysis.
3. Water matrices influenced the drugs' degradation through light-shileding effect.
4. Drugs were not completely mineralized and have slight increasedacute toxicity.
5. Oxidation products were identified and several pathways were first proposed.

✉ Yuan Ren
ceyren@scut.edu.cn

Extended author information available on the last page of the article

also had pharmacological activity (Kosonen and Kronberg 2009; Xu and Lin 2006; Zhuang et al. 2010). To date, the existing work on antihistamines mainly focused on adsorption, biodegradation, and advanced oxidation. Golovko et al. (2020) found that granular activated carbon had a high adsorption capacity for CER and FEX; Faria et al. (2020) indicated that the higher removal efficiency of LOR in EGSB-MBR was attributed to the adsorption and membrane retention, but not biodegradation; Gadipelly et al. (2016) applied the UV/$S_2O_8^{2-}$ system to degrade CER and found that greater than 95% degradation was achieved within 90 min. Since the typical physicochemical and biological processes in traditional WWTPs are designed to remove major pollutants, pharmaceuticals may not be completely removed and are then discharged into the aquatic environment in the effluent. For example, influent and effluent concentrations of CER in a WWTP in Germany were detected at 0.49 µg/L and 0.51 µg/L, and biopersistence was found (Bahlmann et al. 2012). The concentrations of FEX in the influent and effluent of a WWTP in the Czech Republic were 0.18 µg/L and 0.17 µg/L, respectively (Golovko et al. 2014). Antihistamines were also found in the marine environment. CER was found in the Loimi River at approximately 7 ng/L in Finland (Kosonen and Kronberg 2009). The maximum concentration of CER detected in San Francisco Bay was 6.3 ng/L, and the maximum concentration of LOR detected in the Pacific Ocean was 57 ng/L (Nödler et al. 2014). Although concentrations typically in the ng/L to µg/L range have been detected in aquatic environments, the residue of drugs and their pseudo-persistence may cause serious ecological impacts and potential threats to human health (Kostich et al. 2014). LOR in concentrations of hundreds of µg/L could induce 50% mortality of *Ceriodaphnia dubia* (Iesce et al. 2019); FEX at 1.5 µg/L reduced the activity of the damselfly, and the escape time needed from potential predators was extended from 2 to 4 s (Jonsson et al. 2014).

Chlorine oxidation and ultraviolet oxidation are very common tertiary treatment processes in WWTPs; however, their degradation effect and the mechanism thereof on antihistamines are still rarely reported. As an emerging advanced oxidation technology, UV-NaClO combines the advantages of solely using UV or NaClO. In this process, direct photolysis, free radical degradation, and chlorine oxidation were complementary to each other. This enhances the degradation effect of organic compounds to a certain extent and brings great potential applications. UV-NaClO reduced the use of chemical oxidants, thereby reducing the generation of disinfection byproducts and maximizing the safety of the effluent from sewage plants. It could meet the demands of safe effluent under actual conditions and frontier cognition (Aghdam et al. 2017; Wu et al. 2019; Lv 2019).

In this study, three oxidation methods, NaClO oxidation, UV irradiation, and UV-NaClO oxidation, were applied to explore the degradation of three typical structural and functional drugs (LOR, CER, and FEX) and the effects of pH on their removal. We also explored the contribution of different active species to the photolysis process and the effects of different aqueous matrices on UV irradiation and NaClO oxidation. Acute toxicity tests and ultraviolet scans were conducted to estimate the drug degradation reaction system. Based on the UPLC-Q-TOF/MS results, we also proposed the analysis of the oxidation pathways of NaClO on the three drugs and compared the NaClO oxidation and UV photolysis products of CER. We hope that the research results can provide experimental data and a basis for the theoretical analysis of evaluating the removal of drugs in the water environment management and the impact of drugs on the ecosystem.

Materials and Methods

Chemicals

LOR (purity > 98%), CER (purity > 99%), FEX (purity > 98%), methanol, acetonitrile, glacial acetic acid, ammonium acetate, and ammonium dihydrogen phosphate were all chromatographically pure and purchased from Anpel Laboratory Technologies (Shanghai) Inc. (China). H_3PO_4, Na_2HPO_4, KH_2PO_4, NaCl, glycerol, yeast extract, and tryptone were all analytically pure and were purchased from Sinopharm Chemical Reagent Co., Ltd. (China). Sodium thiosulfate was analytically pure and was purchased from Damao (Tianjin) Chemical Reagent Factory (China). Sodium hypochlorite (available chlorine > 10%) was analytically pure and was purchased from Best (Tianjin) Chemical Co., Ltd. (China). $KHCO_3$, KNO_3, humic acid (HA), isopropyl alcohol (IPA), sodium azide (NaN_3), and potassium sorbate (PS) were all of analytical pure and purchased from Aladdin Reagent Co., Ltd. (Shanghai, China).

Experimental methods

NaClO oxidation

To facilitate detection by HPLC, the initial concentrations of the drugs were set at 0.5 mg/L, which is higher than the actual concentration in the aqueous environment. The initial concentration of free chlorine in the NaClO system was 40 mg/L in a 100 ml reaction volume at 25℃. The pH values were adjusted to 3, 5, 7, and 10. Samples were collected at 0, 8, 15, 30, and 60 min and filtered into vials using a syringe filter with an excess of sodium thiosulfate solution to stop the reaction.

UV irradiation

A schematic diagram of the ultraviolet light device is shown in Fig. S1. The initial concentration of each drug was 0.5 mg/L, and the reaction volume was 100 ml with the temperature set at 25℃. The light (125 W medium-pressure mercury lamp, Shanghai Yaming Lighting Company) was turned on and stabilized for 5 min before the experiment. The distance between the liquid surface and light source was 35 cm, and the optical power density was 24 mW/cm^2 (measured by a CEL-NP2000, Beijing Zhongjiaojinyuan Technologies Co. Ltd., Beijing, China). The pH values were adjusted to 3, 5, 7, and 10. Samples were collected at 0, 30, 60, 90, 120, and 150 s and filtered into vials using a syringe filter.

Free radicals quenching

According to the relevant literature (Bodhipaksha et al. 2017), we selected isopropyl alcohol (IPA), sodium azide (NaN_3), and potassium sorbate (PS) to quench the active species produced in the photolysis process: IPA with a concentration (v/v) of 2% was used to quench hydroxyl radicals (·OH), 5 mM NaN_3 was a scavenger for quenching ·OH and singlet oxygen ($^1O_2$), 10 mM PS was used to quench $^1O_2$ and the triplet excited state of the drugs ($^3ANT^*$). Other experimental procedures are described in the Section of UV irradiation.

UV-NaClO oxidation

The reaction conditions were the same as in Section of NaClO oxidationand Section of UV irradation. Samples were collected at the set times (the sampling time of LOR and CER were 0, 30, 60, 90, 120 s; the sampling times of FEX were 0, 10, 20, 30, 40, 50, 60 s) and filtered into a vial using a syringe filter with an excess of sodium thiosulfate solution to stop the reaction.

Influence of different aqueous matrices

We examined the influence of different aqueous matrices on NaClO oxidation and UV irradiation. HCO_3^- (2, 5, 10 mM), NO_3^- (0.2, 0.5, 1 mM), and HA (2, 5, 10 mg/L) were added to the system. Other experimental procedures were described in Section of NaClO oxidation and Section of UV irradiation.

All experiments were conducted in triplicate, and the mean values were used to calculate the degradation efficiencies. The filtered samples were frozen at -20℃ until analysis.

Acute toxicity test

The acute toxicity of the degradation reaction system was tested by *Photobacterium phosphoreum* (purchased from Nanjing Cas Kuake Technology Co., Ltd. China). After activation and cultivation of the freeze-dried powder, the bacterial suspension was used to measure the luminescence intensity of the samples collected during degradation with a multifunctional microplate detection system (BoiTek Cytation 5, USA) according to the method of Li et al. (2021).

Analytical methods

Analysis methods of drugs concentration

The samples were all analyzed by high-performance liquid chromatography (HPLC, LC-20AT, Shimadzu, Japan) equipped with an Eclipse XDB chromatographic column (4.6 mm × 150 mm, 5 μm). The analytical conditions are shown in Table 1.

Ultraviolet scan of degradation products

To determine the cleavage of oxidation products, 5 mL reaction solution was taken at different intervals in the reaction process, and an ultraviolet spectrophotometer (UV7250, Shanghai Longnik Instrument Co., Ltd.) was used to conduct measurements in the range of 200–400 nm. The absorbance of the drug solution treated by NaClO oxidation or UV irradiation was scanned. To increase the detection of drugs, the initial concentrations of the drugs were set at 20 mg/L, and the initial concentration of free chlorine was 100 mg/L.

Table 1 HPLC analytical conditions of the three drugs

Drugs	Mobile phase A/B(V/V)	Detection Wavelength (nm)	Flow rate (mL/min)	LOD [1)] (μg/L)
LOR	0.01 mol/L CH_3COONH_4: acetonitrile = 50:50	247	1	13
FEX	0.005 mol/L $NH_4H_2PO_4$: acetonitrile = 60: 40	220		18
CER	0.005 mol/L $NH_4H_2PO_4$: acetonitrile = 75: 25	230		26

[1)]: LOD: Limit of detection. The detection limit was determined by measuring the same sample 5 times, and 3 times the standard deviation of the measured value was taken as the LOD.

Methods for identification of intermediate products

A UPLC 1290–6540B Q-TOF liquid chromatography–mass spectrometer coupled with an Eclipse plus C18 column (1.8 μm, 2.1 × 100 mm) was used to identify the degradation products of the drugs. The specific conditions were as follows:

Chromatographic conditions: mobile phase: A is methanol, B is water containing 0.2% formic acid; the elution started with 20% methanol, then the methanol concentration increased to 90% within 7 min and was sustained for 1 min, and finally was decreased to 10% within 0.5 min and run for 3.5 min to reach equilibrium before the next injection; injection volume: 10 μL; flow rate: 0.3 mL/min; column temperature: 40℃.

Mass spectrometry conditions: Mass spectrometry was performed in both the positive and negative ionization modes for analysis (ESI ±), and the parameter settings are shown in Table 2.

Calculation methods

Degradation efficiencies

The degradation efficiencies and the first-order reaction kinetics of the three oxidation methods are calculated by Eq. (1) and (2), respectively:

$$Degradation\ efficiency\ (\%) = \frac{(C_0 - C_t)}{C_0} \times 100\% \tag{1}$$

$$ln\frac{C_t}{C_0} = -kt \tag{2}$$

where C_t is the drug concentration at time t, mg/L; C_0 is the initial concentration of the drug, mg/L; k is the first-order kinetic rate constant; and t is the reaction time.

Contribution rates of active species

The contribution rates of active species in the photolysis process can be calculated by Eq. (3), (4), and (5), respectively (Lin et al. 2020):

$$R_{\cdot OH} = \frac{k_w - k_{IPA}}{k_w} \tag{3}$$

$$R_{^1O_2} = \frac{k_{IPA} - k_{NaN_3}}{k_w} \tag{4}$$

$$R_{^3ANT^*} = \frac{k_w - k_{PS}}{k_w} - R_{^1O_2} \tag{5}$$

where $R_{\cdot OH}$, $R_{^1O_2}$, and $R_{^3ANT^*}$ are the contribution rates of ·OH, $^1O_2$, and $^3ANT^*$ to the drugs in the photolysis process; k_{IPA}, k_{NaN_3}, and k_{PS} are the photolysis rate constants after the addition of the quencher IPA, NaN_3, and PS, s^{-1}; and k_w is the actual photolysis rate constant of the drugs in ultrapure water.

Light-shielding coefficients

The light-shielding coefficients of the aqueous matrices are calculated by Eq. (6) and (7). The smaller the total light-shielding coefficients are, the stronger the light shielding effects; when aqueous matrices exist, the theoretical photolysis rate constants of the drugs can be calculated by Eq. (8) (Li et al. 2021):

$$S_\lambda = \frac{1 - \left(10^{-(\alpha_\lambda + \varepsilon_\lambda [ANT])l}\right)}{2.303\left(\alpha_\lambda + \varepsilon_\lambda [ANT]\right)l} \tag{6}$$

$$\sum_{200}^{400} S_\lambda \frac{\sum L_\lambda S_\lambda \varepsilon_\lambda}{\sum L_\lambda \varepsilon_\lambda} \tag{7}$$

$$k' = k_w \bullet \sum_{200}^{400} S_\lambda \tag{8}$$

where S_λ represents the light-shielding coefficient of the aqueous matrices (HCO_3^-, NO_3^-, and HA) at wavelength λ; $\sum_{200}^{400} S_\lambda$ represents the total light-shielding coefficient with a wavelength range of 200–400 nm; *[ANT]* represents the concentration of the drugs; a_λ represents the absorbance of the aqueous matrices at wavelength λ; ϵ_λ represents the molar absorption coefficient of the drugs at wavelength λ; l represents the light path; L_λ represents the percentage of light intensity of the mercury lamp; and k' is the theoretical photolysis rate constant of the drugs.

Table 2 Mass spectrometry parameter settings

Parameter	Gas temp	Gas flow	Sheath gas temp	Sheath gas flow	Nebulizer	Nozzle voltage
Value	300℃	8 L/min	350℃	10 mL/min	45 psi	1000 V

Acute toxicity

Acute toxicity is assessed by the relative luminescence intensity (*RLI*), which can be calculated by Eq. (9).

$$RLI = \frac{L_t}{L_0} \times 100\% \quad (9)$$

where L_t is the luminous intensity at time t and L_0 is the initial luminous intensity.

Results and discussions

Degradation effects of NaClO on the three drugs

The pH value is an important water quality parameter in the water treatment process. The existence of drugs and free chlorine may change at different pH levels, resulting in differences in degradation efficiencies. The acidity coefficients (p*K*a) of HOCl and the three drugs were as follows: HOCl (p*K*a = 7.54), LOR (p*K*a = 4.3), FEX (pK_{a_1} = 4.2, pK_{a_2} = 9.52), and CER (pK_{a_1} = 2.1, pK_{a_2} = 8). The degradation of the three drugs by NaClO at different pH values is shown in Fig. 1.

(1) LOR

As shown in Fig. 1, slight degradation of LOR by NaClO was observed after 1 h. The degradation efficiencies ranged from 3%–11%, which decreased with increase in pH. When pH < 4.3, LOR was mainly in the molecular form, while LOR^- was mainly in the ionic form when pH > 4.3. Because HOCl is a weak acid, the dominant form is HOCl at pH < 7.54 and in the form of OCl^- at pH > 7.54 (Ji et al. 2016). When the pH was in the range of 7–10, the solution was dominated by LOR^- and OCl^-. More energy was needed for the collision of charge-repelled anions, and a less effective impact reduced the degradation efficiency of LOR (Yan et al. 2017). When the pH was 3 and 5, the dominant forms in the solution were HOCl and LOR and HOCl and LOR^-, respectively. HOCl is more electrophilic than OCl^-. Therefore, the degradation efficiencies of LOR were higher under acidic conditions. In addition, we speculated that HOCl had a stronger oxidation effect on LOR, so when pH = 3, the degradation effect of LOR was more obvious than that at pH = 5.

(2) FEX

For FEX, the reactivity of FEX under alkaline conditions was much higher than that under acidic conditions. The degradation efficiencies increased significantly from 11 to 92% in 1 h with increase in pH, especially from pH = 5 to pH = 10. Because FEX is a zwitterionic compound, the carboxyl group on FEX was gradually ionized and lost protons to form -COO^- as the pH increased. The ionized form of the carboxyl group may increase the sensitivity of FEX (Gumieniczek et al. 2019), and it was also reported that deprotonated ions were more susceptible to the attack of electrophiles HOCl and ClO^- (Gallard and von Gunten 2002). The reasons given above explain why the ability of FEX to react with chlorine was enhanced.

(3) CER

For CER, which is also a zwitterionic compound, the reasons for its high degradation efficiencies under alkaline conditions were the same as that of FEX. In particular, the degradation efficiency of CER reached 85% in 1 h at pH = 3. HOCl was dominant in the solution at that time, and the piperazine ring, with a higher electron density on the CER molecular structure, was the best position for the electrophilic reagent to attack (Dodd et al. 2005; Pan et al. 2021), leading good degradation effect under acidic conditions.

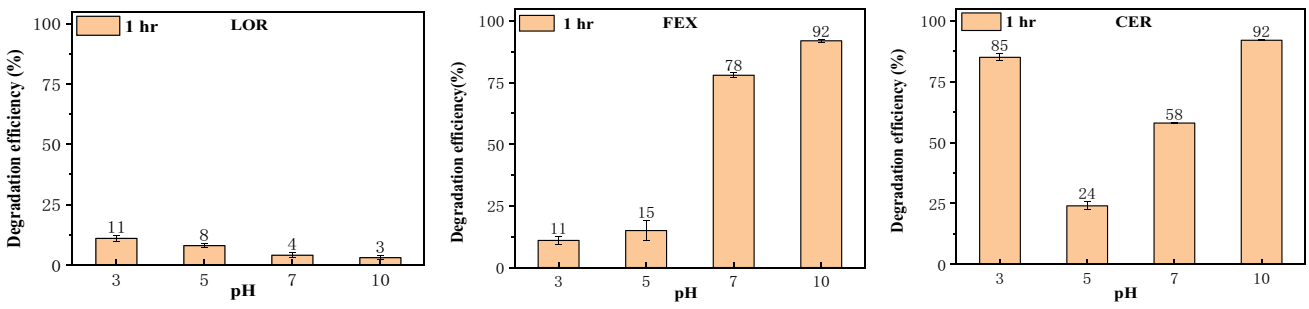

Fig. 1 Degradation efficiencies of drugs with NaClO at different pH values

Degradation effects of UV irradiation on the three drugs

At different pH values, the degradation effects of the three drugs oxidized by UV irradiation are shown in Fig. 2.

As shown in Fig. 2, UV irradiation had more efficient degradation for these three drugs than NaClO oxidation. When pH = 7, the degradation efficiencies at 150 s were all greater than 75%. The three drugs are photosensitive organics with poor stability under UV irradiation (Abounassif et al. 2005; Bergheim et al. 2014; Breier et al. 2008). In addition, other antihistamines, such as ebastine, terfenadine, and levocetirizine, all had good photosensitivity according to the literature, and these drugs also contain nitrogen-containing heterocycles (Gumieniczek et al. 2019; Tarozzi et al. 2003; Gunjal et al. 2011). Boreen et al. (2003) found that many macrolide antibiotics without chromogenic functional groups limited the photochemical reactions. Therefore, it was speculated that chromophoric groups such as the nitrogen-containing heterocycles contained in these three drugs promoted their photoreactivity. The degradation efficiencies of LOR were significantly increased from 9 to 93% in 150 s when the pH increased from 3 to 7. This was because the anionic form of LOR increased with increase in pH, thus promoting the attack by ·OH with strong electrophilicity and degradation effects (Ji et al. 2012a). When the pH was 10, the degradation efficiency of LOR decreased slightly because singlet oxygen generation was inhibited due to the increase in hydroxide concentration in the solution (Bilski et al. 1996). Different from LOR, pH had less effect on the photolysis of FEX and CER, but the removal efficiencies were above 75%, indicating that UV irradiation had a good degradation effect on the different existing forms of FEX and CER.

Degradation effects of UV-NaClO on the three drugs

The degradation effects of the three drugs oxidized by UV-NaClO at different pH values are shown in Fig. 3. As shown in Fig. 3, under the UV-NaClO system, the degradation efficiencies of LOR increased from 33 to 85% with the increase in pH from 3 to 10. When the pH values were 3 and 5, the degradation efficiencies of FEX at 60 s were 62% and 93%, respectively. When pH = 7 and pH = 10, FEX reached a complete degradation within 20 s. The degradation efficiencies of the two drugs under alkaline conditions were greater than those under acidic conditions. However, CER showed the best degradation effect under acidic conditions. UV-NaClO oxidation had a great degradation effect on drugs because of its synergistic effect on the degradation of organic compounds (Fang et al. 2014). Under UV irradiation, free chlorine produced active species (Formulas S1–S5), such as chlorine free radicals (Cl·), superoxide anions ($O\cdot^{-}$), and hydroxyl free radicals (HO·) (Dong et al.

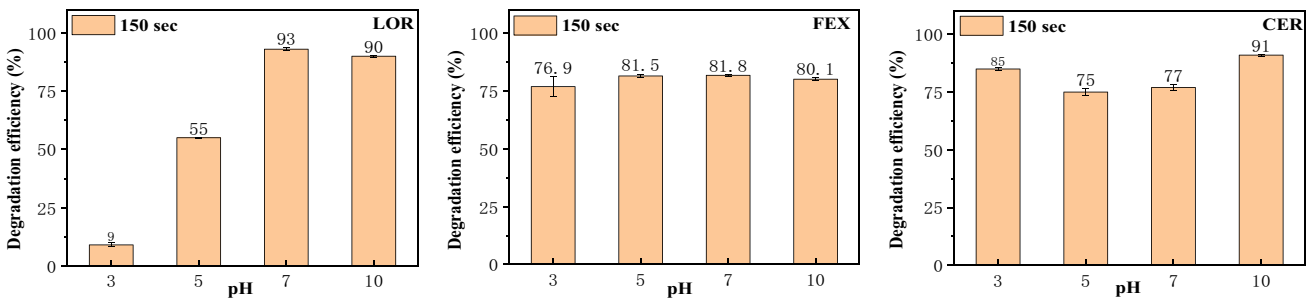

Fig. 2 Degradation efficiencies of drugs with UV light at different pH values

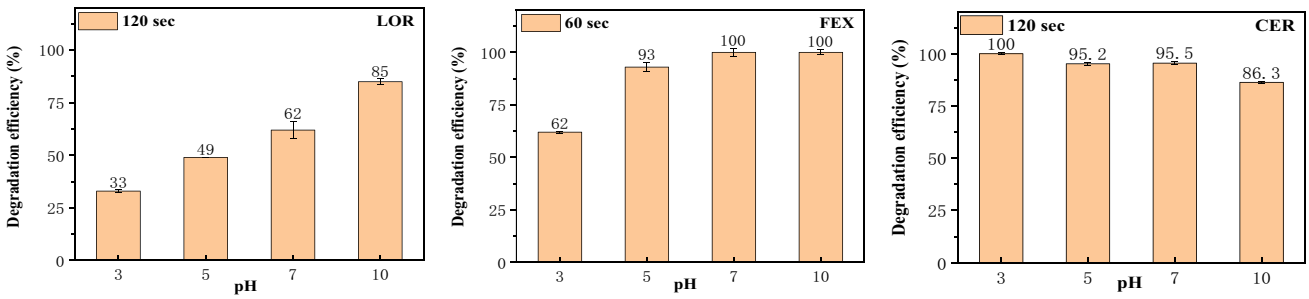

Fig. 3 Degradation efficiencies of drugs with UV-NaClO at different pH values

2017), thus enhancing the degradation effect of organic compounds. In addition, we found that the change in the drugs in the UV-NaClO system was similar to that in the UV system under different pH conditions. UV irradiation played a leading role in the combination of UV and NaClO.

Comparison of degradation kinetics of the three oxidation methods

Under different pH conditions, drugs were oxidized by the three oxidation methods, all following the first-order kinetic equation (Fig. S2–S4). The rate constants are shown in Table 3. By comparing the data in Table 3, we found that UV-NaClO oxidation had the best degradation effect on drugs under most conditions. In addition, a few special considerations are discussed below.

The rate constants of LOR in different treatments at pH 5 and 7 were ranked as follows: UV > UV-NaClO > NaClO. The removal effect of UV-NaClO was not as good as that of UV, which may indicate that the degradation efficiencies of LOR by NaClO were too small and could be ignored during the reaction time of 120 s. In contrast, the free chlorine in the solution produced by NaClO competed with LOR to absorb photons. A previous report showed that the ability of free chlorine to absorb photons was much greater than that of organic compounds (Jiang et al. 2018). That is why the removal efficiencies of UV-NaClO on LOR at pH 5 and 7 were not as high as those of UV irradiation alone.

Another point worth noting was that CER achieved the maximum degradation efficiencies in both UV-alone and NaClO-alone systems at pH 10. However, in the UV-NaClO system, the degradation at pH 10 was not the best as expected, which eventually led to rate constants ranked as UV > UV-NaClO > NaClO. Different from the above analysis of LOR, the effect of NaClO on CER could not be ignored. Therefore, in the UV-NaClO system, the reasons for the poor effect of CER when pH = 10 were as follows: 1) The quantum yield of HOCl was higher than that of OCl^-. When the pH was increased to 10, the main component of free chlorine changed from HOCl to OCl^-, and the reduction in the quantum yield reduced the generation of ·OH and Cl. 2) The degradation rate constants of HOCl and OCl^- reacting with ·OH were 2.0×10^9 L/(mol·sec) and 8.8×10^9 L/(mol·sec), respectively. The scavenging effect of OCl^- on ·OH was greater than that of HOCl. Therefore, lower degradation of CER was observed at pH 10 (Wu et al. 2016).

Table 3 Oxidation rate constants of the three oxidation methods

Drugs	pH	Degradation rate constants		
		NaClO (min^{-1})	UV (s^{-1})	UV-NaClO (sec^{-1})
LOR (R^2 = 0.980–0.999)	3	0.0018	0.0006	0.0030
	5	0.0015	0.0052	0.0045
	7	0.0007	0.0186	0.0064
	10	0.0005	0.0155	0.0157
FEX (R^2 = 0.981–0.999)	3	0.0017	0.0090	0.0150
	5	0.0024	0.0109	0.0328
	7	0.027	0.0116	/ *
	10	0.047	0.0107	/ *
CER (R^2 = 0.985–0.999)	3	0.0292	0.0124	0.0341
	5	0.0045	0.0093	0.0225
	7	0.0127	0.0093	0.0282
	10	0.0391	0.0163	0.0151

*: When pH = 7 and 10, FEX reacted too fast and was completely degraded within 20 s, which could not be measured. Therefore, only the data with pH values of 3 and 5 are retained in Table 3.

Contribution rates of the active species in photolysis

Comparing UV-NaClO oxidation and UV irradiation, there was no significant difference in drug removal between the two treatments. We investigated the free radicals generated in the UV system to explore their contribution rates during the degradation process.

Photolysis was divided into two processes: direct photolysis and indirect photolysis. In the former, the compound directly absorbed photons; the latter was a reaction between the compound and the various active species produced by photosensitization (Ozaki et al. 2021). As seen from Table 4, the contribution rates of $^1O_2$ for FEX and CER reached 70%, indicating that both drugs mainly underwent indirect photolysis guided by $^1O_2$. In addition, we found that the contribution rates of active oxygen species to these two drugs were relatively similar. This is because CER and FEX are zwitterionic compounds containing carboxyl groups and have relatively similar molecular structures. For LOR, the contribution rates of $^1O_2$ and $^3ANT^*$ were relatively close, which meant that the direct photolysis and indirect photolysis of LOR were on the same level. According to the above analysis, the three active species were involved in the photolysis process, and the mechanism was speculated as follows: ANT absorbed the photons to obtain energy and then was transformed into $^3ANT^*$ to undergo direct photolysis; $^3ANT^*$ transferred part of the energy to $^3O_2$, the ground state form of dissolved oxygen in water, to excite active $^1O_2$. Then, $^3O_2$ accepted the electrons transferred from the organic

Table 4 Contribution rates of the active species in photolysis

Drugs	$^1O_2$	$^3ANT^*$	·OH
LOR	46.2%	49.7%	14.6%
FEX	70.1%	28.9%	10.9%
CER	70.1%	27.9%	2.05%

compounds to produce H_2O_2, which absorbed photons to produce ·OH (Derbalah et al. 2020; Ping et al. 2021).

The influence of aqueous matrices on NaOCl oxidation and UV irradiation

In natural water bodies and wastewater, many different aqueous matrices will affect oxidation and degradation efficiency due to stimulation, inhibition, or shielding effects (Lin et al. 2020). HCO_3^-, NO_3^-, and HA were selected to estimate their effect in the process of drug degradation, and the results of NaClO oxidation are shown in Fig. 4.

HCO_3^- promoted drug degradation because it could generate $CO_3\cdot^-$, which had stronger oxidizing properties. With the addition of NO_3^- and HA, they had a promoting effect on the degradation of FEX but had an inhibitory effect on the degradation of CER. For HA, the two different results may be because HA containing a large number of active groups could compete with the drugs for the available chlorine in the system, resulting in a decrease in the degradation efficiencies of the drugs. On the other hand, HA had good adsorption properties that could lead to great removal efficiencies of the drugs.

Figure 5 shows the effects of different aqueous matrices on degradation efficiencies, and Table 5 lists the kinetics parameters of the photolysis process.

From Table 5, we can find that the total light-shielding coefficients of different aqueous matrices were all less than 1, indicating that the addition of aqueous matrices had light-shielding effects on the photolysis of drugs. However, k' and k were not equal, indicating that the aqueous matrices not only affected the photolysis process through the light-shielding effect but also through the removal and excitation of active species (Ping et al. 2021). Combining Fig. 5 and Table 5, the degradation efficiencies showed slight fluctuations with the addition of HCO_3^-. For LOR and FEX, HCO_3^- was a scavenger of ·OH, which reduced the amount of ·OH and had inhibitory effects on their

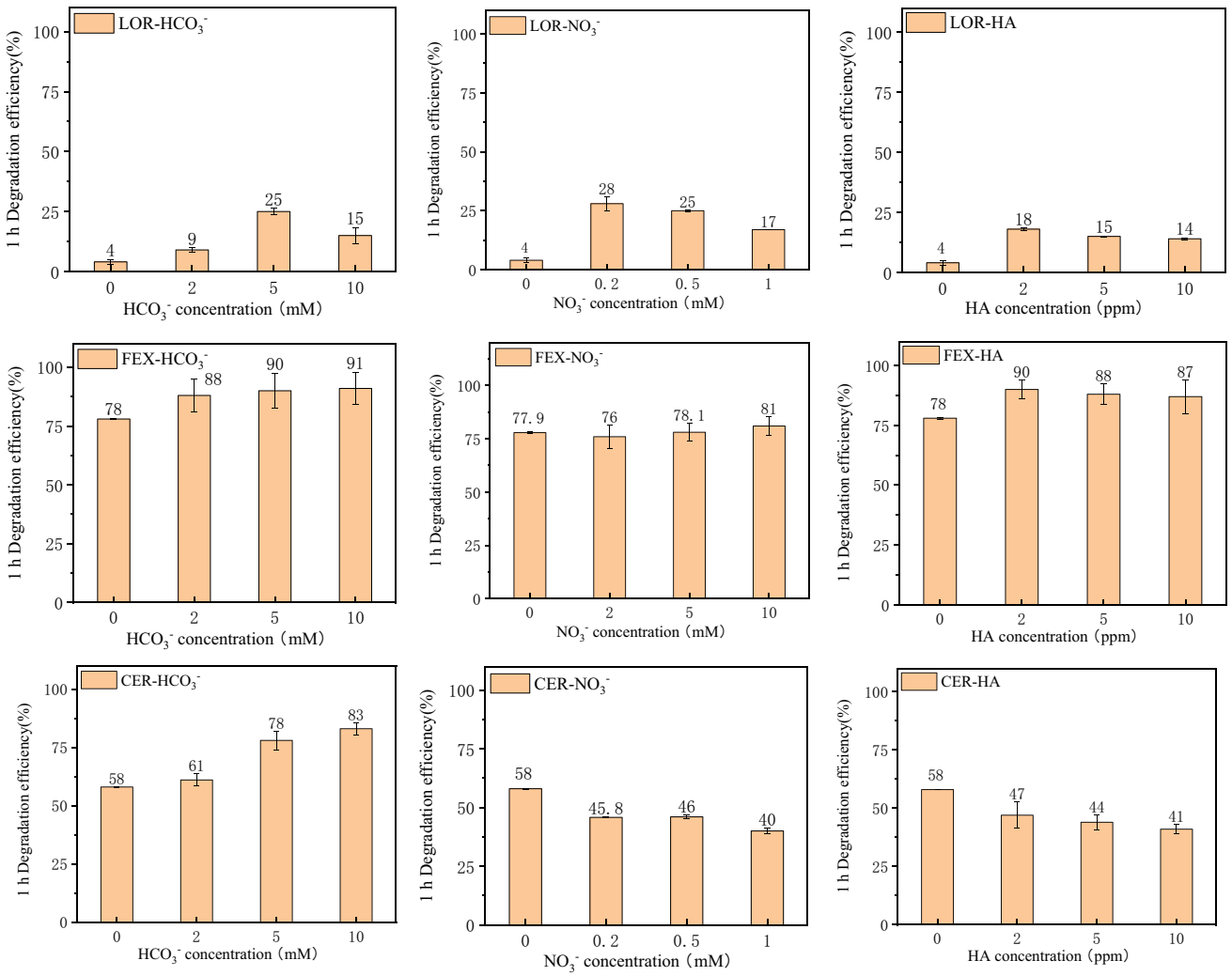

Fig. 4 The influence of aqueous matrices on NaOCl oxidation

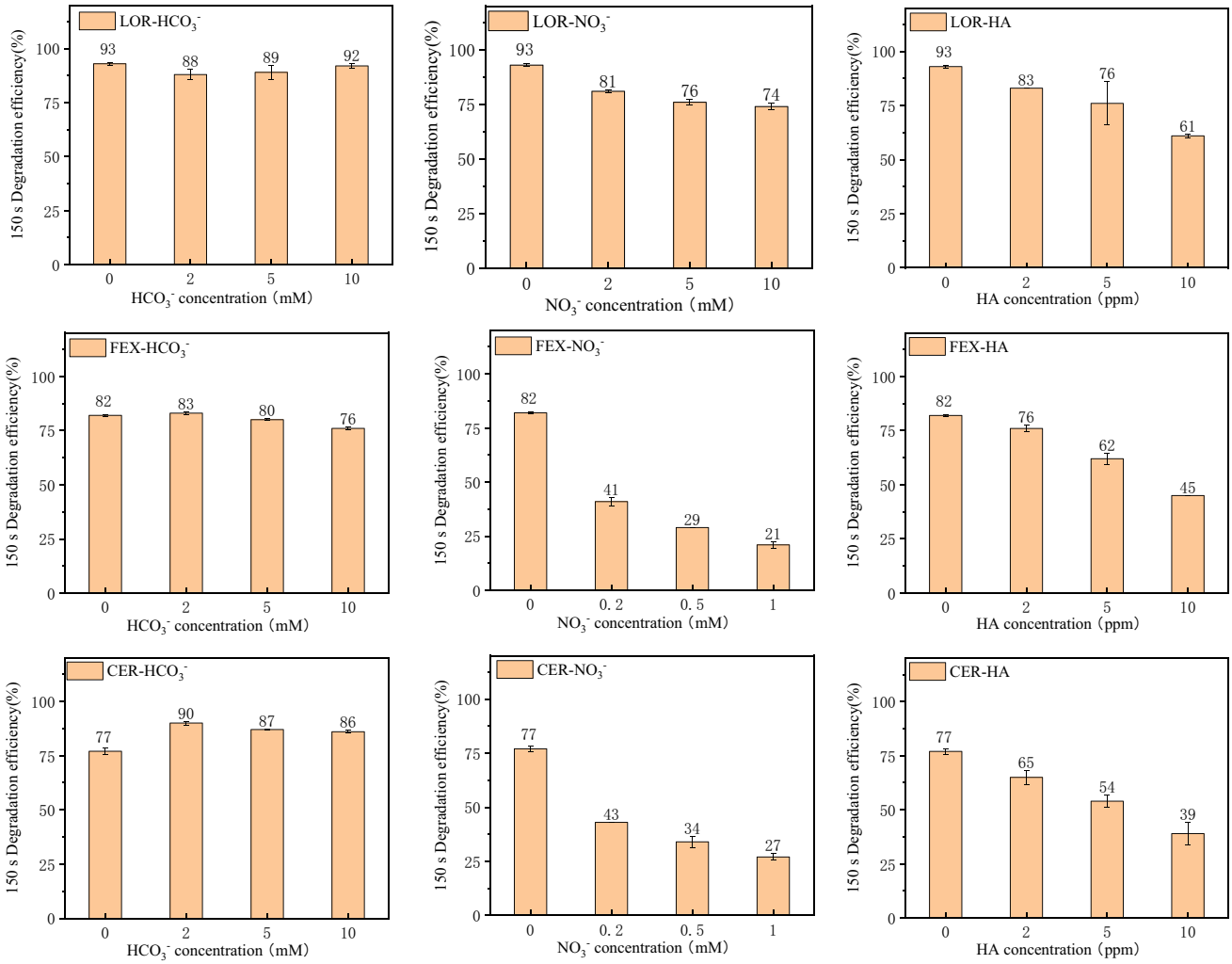

Fig. 5 The influence of aqueous matrices on UV irradiation

degradation. (Formula S6) (Lin et al. 2020). In addition, we found that the contribution rates of ·OH were relatively low and that the addition of HCO_3^- did not have significant inhibitory effects on the drugs. For CER, the addition of HCO_3^- actually promoted the reaction because HCO_3^- produced $CO_3\cdot^-$ under ultraviolet irradiation, which had a better degradation effect on CER (Ji et al. 2012b).

We clearly observed that NO_3^- and HA had significant inhibitory effects on photolysis, and the degradation efficiencies decreased as the concentrations of NO_3^- and HA increased. With the decrease in the total light-shielding coefficient, the shielding effects of NO_3^- and HA on the photolysis of the drugs will be greater. The addition of NO_3^- and HA could compete with the drugs for the absorption of photons, and the decrease in absorbable photons resulted in lower degradation efficiencies. The inhibitory mechanisms of HA can react with $ANT\cdot^+$ produced by the reaction of ANT and free radicals, and $ANT\cdot^+$ is then transformed to the parent form (ANT) (Formulas S7-S8) (Wang et al. 2017).

Acute toxicity changes of the drugs

The samples were collected at intervals to test the acute toxicities of the three drugs, and the results are shown in Fig. 6.

Figure 6 shows that the luminous intensity showed a weakening trend in most cases, indicating that the toxicity of the drug degradation intermediates was greater than that of their parent drugs. For a certain point in time, the increase in relative luminous intensity was due to the generation of electrophilic groups such as carbonyl groups during the degradation process, which led to reduced toxicity (Cronin et al. 2001). Some research has reported the overall toxicity of antihistamines: Gadipelly et al. (2016) studied the luminescence intensity of *Photobacterium phosphoreum* in samples taken at different time intervals during the degradation

Table 5 Total light-shielding effects of different aqueous matrices

Drugs	Aqueous matrices	Concentration	$\sum_{200}^{400} S_\lambda$	k' (sec^{-1})	k (sec^{-1})	k/k_w [4)]
LOR	Pure water	0	1	0.01859	0.01859 [1)]	1
	HCO_3^- (mM)	2	0.974	0.01810	0.01610	0.866
		5	0.969	0.01802	0.01683	0.905
		10	0.963	0.01789	0.01675	0.901
	NO_3^- (mM)	0.2	0.891	0.01660	0.01084	0.583
		0.5	0.859	0.01597	0.00859	0.462
		1	0.832	0.01546	0.00781	0.420
	HA (mg/L)	2	0.879	0.01633	0.01185	0.637
		5	0.754	0.01402	0.00908	0.488
		10	0.604	0.01122	0.00693	0.373
FEX	Pure water	0	1	0.01156	0.01156 [2)]	1
	HCO_3^- (mM)	2	0.958	0.01084	0.01145	0.990
		5	0.94	0.01063	0.01087	0.940
		10	0.911	0.01031	0.00955	0.826
	NO_3^- (mM)	0.2	0.571	0.00646	0.00338	0.292
		0.5	0.458	0.00518	0.00227	0.196
		1	0.401	0.00453	0.00156	0.135
	HA (mg/L)	2	0.859	0.00972	0.00957	0.828
		5	0.727	0.00822	0.00592	0.512
		10	0.575	0.00650	0.00400	0.346
CER	Pure water	0	1	0.00929	0.00929 [3)]	1
	HCO_3^- (mM)	2	0.961	0.00893	0.01516	1.632
		5	0.944	0.00877	0.01362	1.466
		10	0.918	0.00853	0.01271	1.368
	NO_3^- (mM)	0.2	0.619	0.00575	0.00376	0.405
		0.5	0.513	0.00476	0.00274	0.295
		1	0.451	0.00419	0.00197	0.212
	HA (mg/L)	2	0.861	0.00780	0.00790	0.850
		5	0.727	0.00675	0.00474	0.510
		10	0.573	0.00533	0.00347	0.374

$\sum_{200}^{400} S_\lambda$: Total light-shielding coefficient; k': theoretical photolysis rate constant; k: actual photolysis rate constant.

[1)], [2)], [3)]: Actual photolysis rate constant of the drugs in ultrapure water, k_w.

[4)]: When $k/k_w > 1$, the aqueous matrix promotes the reaction; otherwise, the reaction is inhibited.

of CER by UV/$S_2O_8^{2-}$ and found that the toxicities of the samples first increased and then decreased; Borowska et al. (2016) found that the ozone-treated FEX sample (containing parent drugs and the products) inhibited the luminosity of *Aliivibrio fischeri* by 10%. The previous results and this study indicated that the toxicity of advanced oxidation needs more consideration. In the two systems, NaClO and NaClO-UV, the degree of toxicity of the samples was greater than that in the UV system. It was speculated that the addition of NaClO resulted in the generation of disinfection byproducts, which were highly toxic to luminescent bacteria. Based on our research, UV had the advantages of high disinfection efficiency and high safety. Therefore, we recommend the use of the UV method in actual projects.

Drugs degradation intermediates and pathways

Figure 7 shows the UV spectrum of the drug solution over time by NaClO oxidation and UV irradiation. The characteristic absorption peaks of LOR, FEX, and CER were approximately at 247 nm, 220 nm, and 230 nm, respectively. As the reaction proceeded, the absorbance of the three drugs at the characteristic absorption peaks gradually weakened, but new absorption peaks appeared. This indicated that the drugs were transformed into their degradation products but not completely mineralized during this process. Comparing NaClO oxidation and UV irradiation, it was found that not only did UV irradiation have stronger effects on drug degradation but also the wavelengths of the new absorption peaks

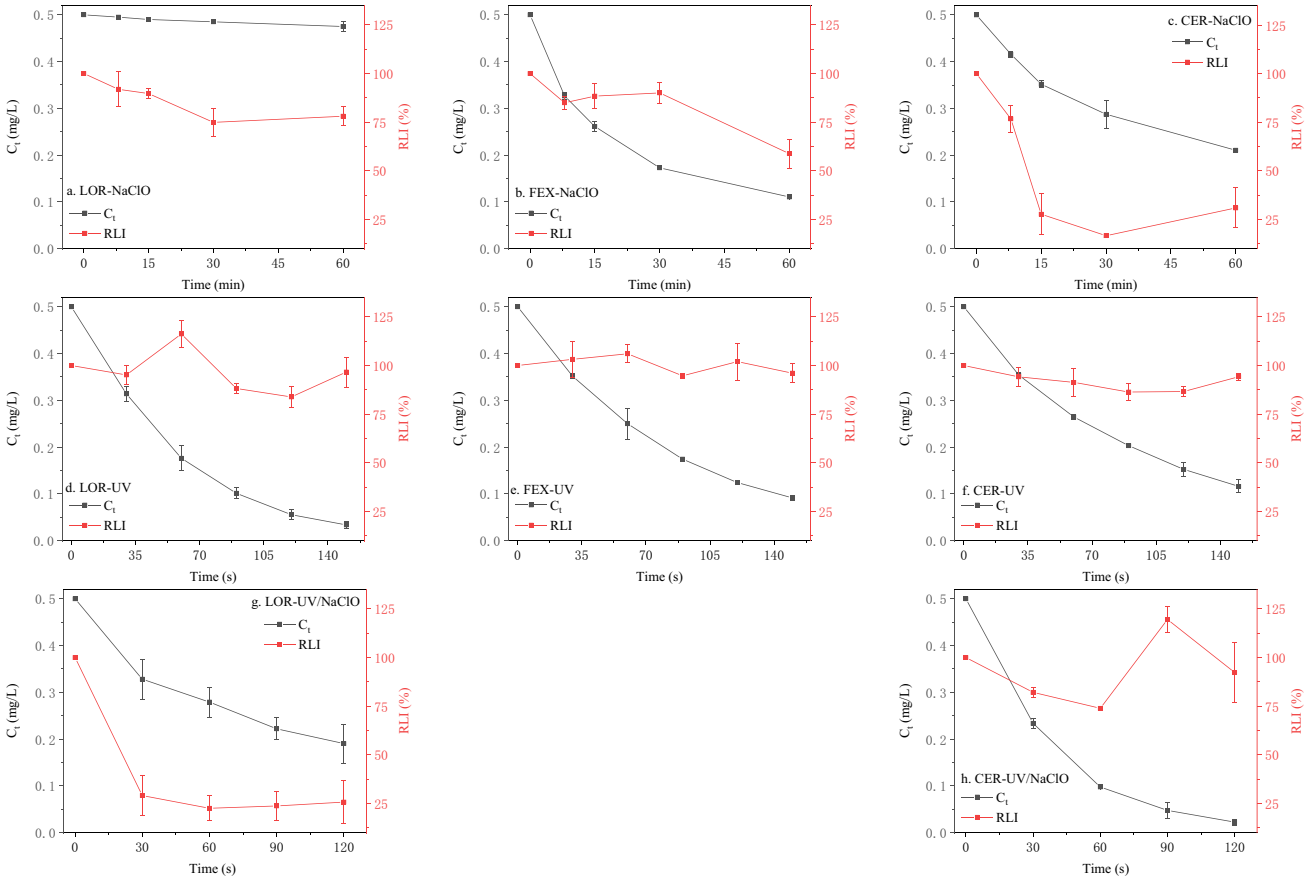

Fig. 6 Acute toxicity of drugs in different oxidation systems (When pH = 7, FEX reacted too fast and was completely degraded within 20 s, so we did not measure the acute toxicity of FEX in the UV-NaClO system.)

generated by the oxidation of NaClO (at approximately 300 nm) were greater than those produced by UV irradiation (at approximately 250–270 nm). This was because the strongly oxidizable electrophiles such as hypochlorous acid and hypochlorite present in the NaClO solution system could react with the drugs to form chlorinated products. When chlorine atoms containing n electrons were connected with the ring, they could form a conjugated system that enhanced the color generation ability of the ring and caused the ultraviolet absorption to move to 300 nm in the redshift direction (Cai et al. 2013; Zhang et al. 2014).

Since UV scanning only gave macroscopic signals of drugs with functional groups such as benzene rings, their specific degradation pathways need tobe inferred by identifying their degradation products. The photolysis products of LOR and FEX were reported in previous articles (Iesce et al. 2019; Breier et al. 2008). Therefore, this study only identified the photolysis products of CER and the NaClO oxidation products of these three drugs.

Both primary and secondary mass spectrometry are widely used to analyze the molecular structure of intermediates (Soufan et al. 2013; Vione et al. 2009; Yassine et al. 2017). According to the results of MS1 and MS2 given by Q-TOF, some potential structures of the intermediates are presented (Table. S1-S4) and the degradation pathways are proposed.

(1) NaClO oxidative degradation pathways of LOR (as shown in Fig. 8)

Pathways I and II As a functional group rich in electron groups, the carbon–carbon double bond (C = C) is vulnerable to attack by electrophiles. Therefore, the C = C in the LOR molecule was oxidized and cracked to form a ketone (Yu and Zhao 2019), forming cpd-1. cpd-2 was found to be an isomer of the LOR molecule, and the unsaturated double bond could react with HOCl to form cpd-3.

Pathway III It was speculated that cpd-4 was produced from the rupture of the bond between C_1 and C_2 of LOR. cpd-5 was formed by the further breaking of the C–Cl bond and the O_3-C_2 bond in the cpd-4 molecule. Armaković et al. (2016) calculated that the C–Cl bond dissociation energy (BDE) for LOR was

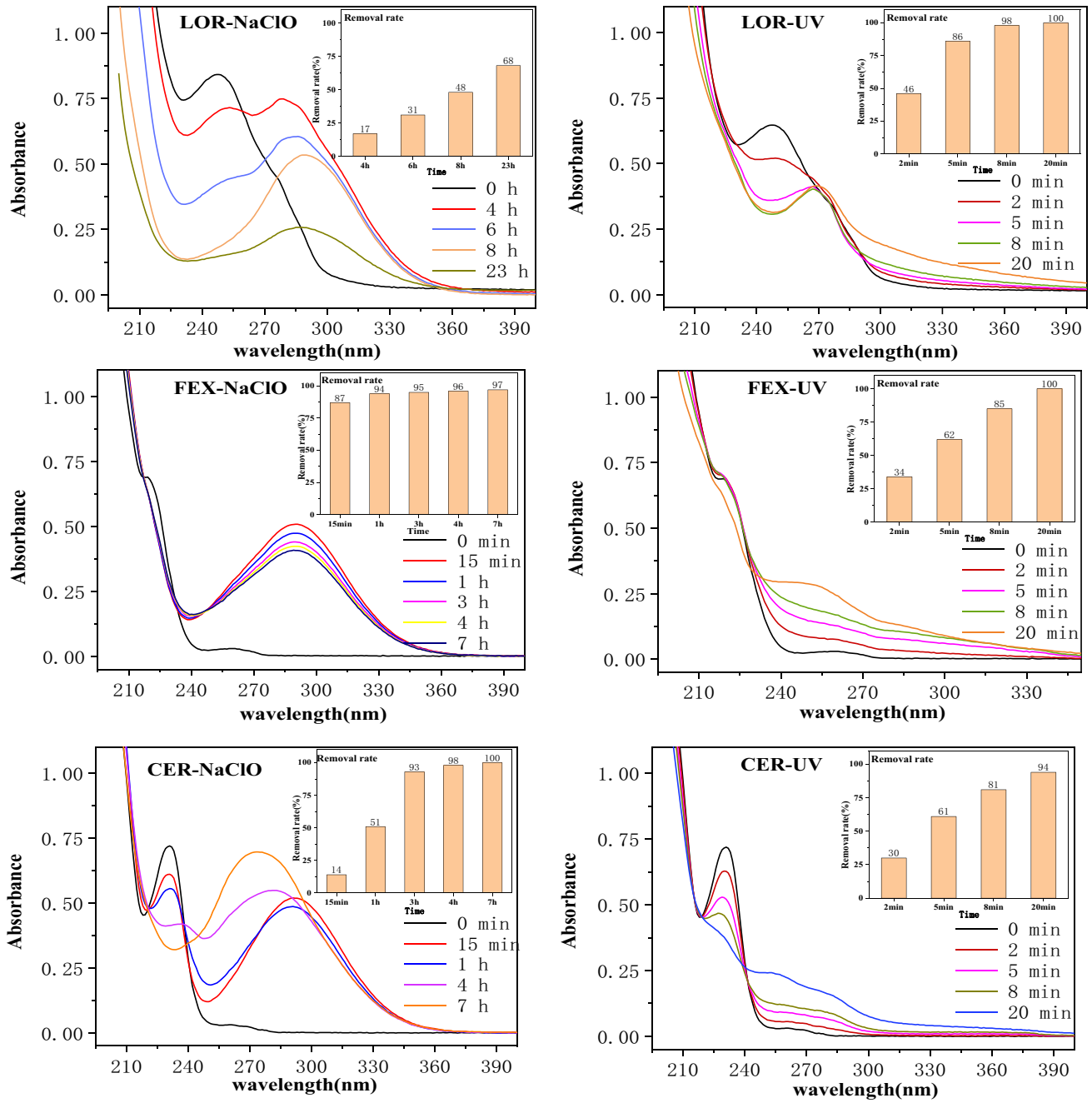

Fig. 7 Evolution of the UV spectrum of the drug solution over time during NaClO oxidation and UV irradiation

91.26 kcal/mol. Their study also showed that the aliphatic part of LOR was prone to bond rupture, and the BDEs between C_1 and C_2 and between O_3 and C_2 were relatively low, among which the weakest bond existed between O_3 and C_2. Therefore, we speculated that pathway III was the dominant pathway. In addition, the cpd-5 molecule was further decarboxylated to form cpd-6 due to the instability of the carbamate. Desloratadine, the human metabolite of LOR, was not found in the product identification. This may be due to the C–Cl bond fracture of desloratadine, which promoted the formation of cpd-6 in another way.

Pathway IV In the process of degrading organic compounds with NaClO, chlorine atoms may be replaced by hydroxyl groups to form cpd-7, and further fracture of O_3-C_2 occurred to form cpd-8. In addition, cpd-5 may be formed due to the occurrence of side-chain fracture of cpd-8 during the reaction, which was another possible formation process of cpd-5. As an electron donor group, phenolic hydroxyl groups enriched with electrons facilitated substitution reactions between phenolic compounds and electrophiles such as HOCl (Liu et al. 2012). It was speculated that the chlorine

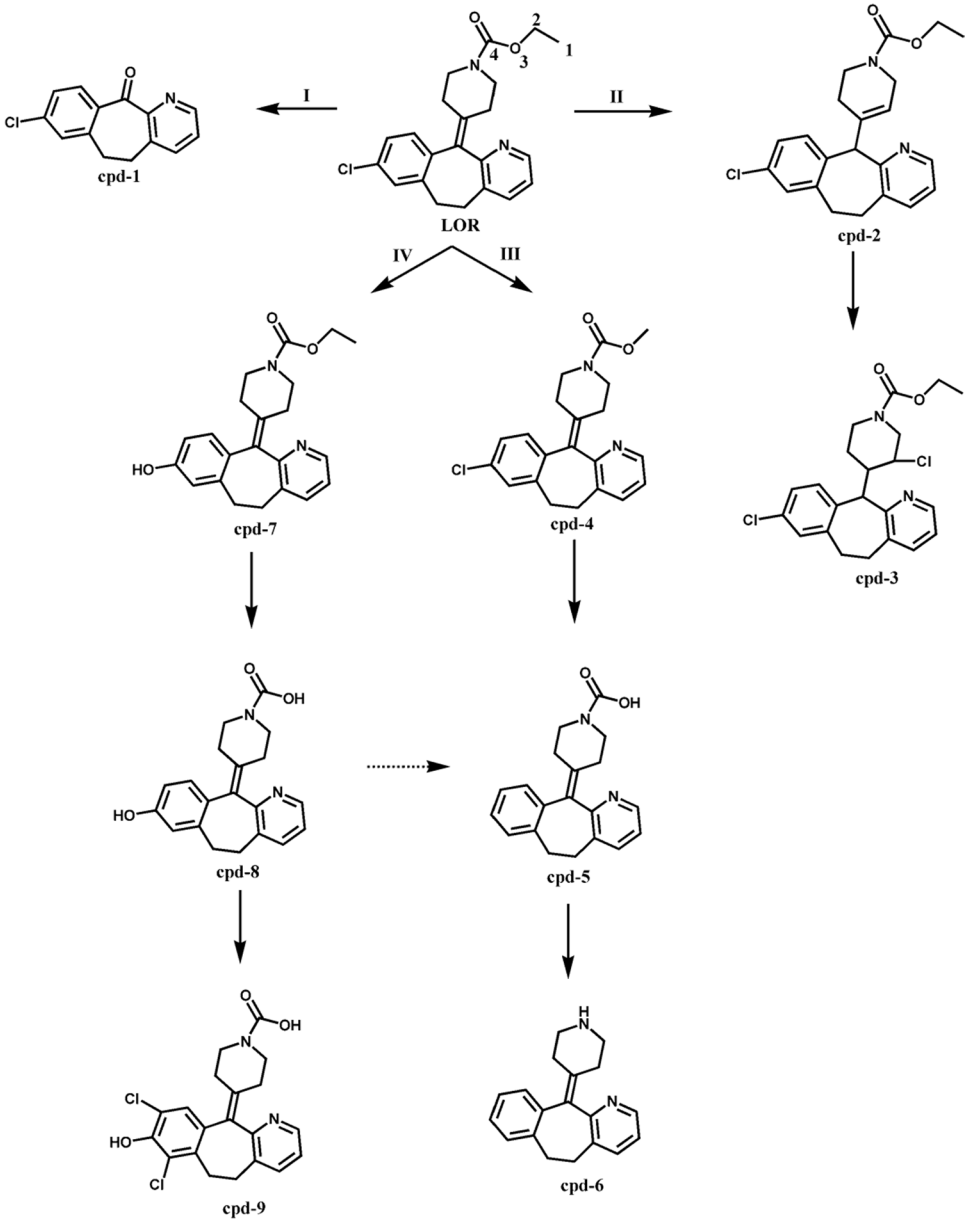

Fig. 8 Possible degradation pathways of LOR oxidized by NaClO

in hypochlorous acid molecules attacked the positively charged carbon on the benzene ring and generated a variety of chlorine-substituted phenols (Hu et al. 2002). Therefore, a chlorine substitution reaction could occur in the benzene ring to generate compound cpd-9.

(2) NaClO oxidative degradation pathways of FEX (as shown in Fig. 9)

Pathway I There is a tertiary amine in the FEX molecule, and pathway I may be the dominant. Nitrogen in organic compounds was the main site for possible attack by oxidizing agents (Dyakonov et al. 2010). The oxidant attacked the tertiary amine nitrogen to form nitrogen oxide during the reaction, namely cpd-1. Then, cpd-1 was oxidized to a ketone to form cpd-2 with 2 Da less in the molecule.

Pathway II cpd-3 was formed by the removal of two methyl groups from the FEX molecule. It was reported that certain types of substrates (various monohydroxybenzoic acid species) underwent halogenated decarboxylation during chlorination. This reaction was attributed to the direct action of the hydroxyl groups in the substrate structure on the carbon atoms of the carboxyl groups (Larson and Rockwell 1979). Therefore, decarboxylation and demethylation reactions

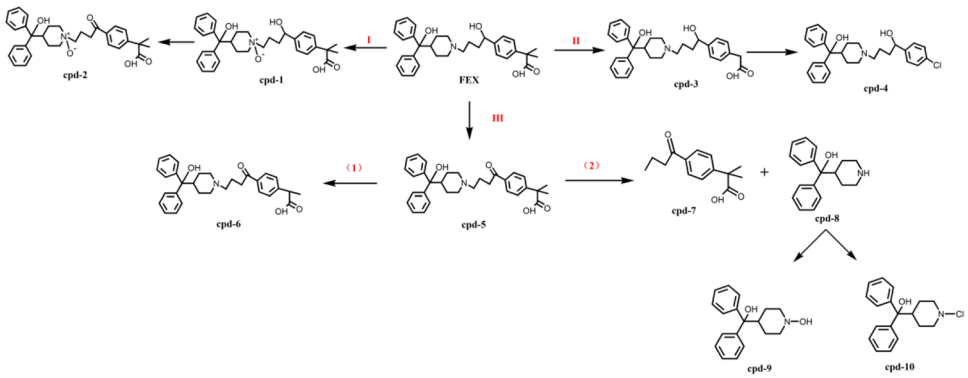

Fig. 9 Possible degradation pathways of FEX oxidized by NaClO

occurred in cpd-3, and the part that is removed may be replaced by chlorine to form cpd-4.

Pathway III Product cpd-5 was obtained by oxidizing the secondary hydroxyl group in the FEX molecule to form a benzoyl group (Henning et al. 2019). It was further speculated that cpd-5 underwent two processes: (1) demethylation to produce cpd-6, and (2) dealkylation of the tertiary amine to form cpd-7 and cpd-8. The hydroxylation reaction may occur during the chlorination process (Yang et al. 2019), leading to the formation of cpd-9, or chlorine attacking the amine functional group to form cpd-10. The reaction efficiency of a secondary amine and HOCl is much higher than that of a tertiary amine and HOCl (Boreen et al. 2003), so the formation of cpd-10 more easily occurred.

(3) NaClO oxidative degradation and photolysis pathways of CER (shown in Fig. 10 and Fig. 11, respectively)

Due to its strong oxidation capacity and structural characteristics, NaClO mainly reacts with organic compounds by oxidation, addition to unsaturated bonds, and electrophilic substitution (Ji et al. 2016). However, the degradation mechanisms of photolysis were completely different from those of NaClO oxidation. After absorbing photons, the substance was excited into a triple excited state, which was not stable. The products were then formed through reactions such as cracking and hydrogen extraction. In addition, light could produce active species such as $^1O_2$ and HO·, which could form products through hydroxylation, ketonization, and other reactions (Gligorovski et al. 2015).

By comparing the products in Fig. 10 and Fig. 11, we found that the NaClO oxidative degradation and photolysis process of CER produced three groups of the same degradation products: cpd-1 and UV-1, cpd-2 and UV-2, and cpd-5 and UV-3.

For the first and second groups of the same products, cpd-1 and UV-1, cpd-2 and UV-2, their generation processes were different: in the chlorine oxidation process (Pathway Cl-I), C-N bond fracture occurred on the tertiary amine of CER, and the dealkylation of N_1-amine led to the formation of carbonyl compounds and secondary amines, forming cpd-1 and cpd-2. In the photolysis process (UV-I), $^1O_2$ generated in the aqueous solution attacked the tertiary amine in the CER molecule, resulting in the production of UV-1 and UV-2. From the previous analysis, $^1O_2$ played the more obvious role in the photolysis of CER than $^3ANT^*$ and ·OH, so it could be inferred that UV-I was the main degradation reaction in the process of photolysis.

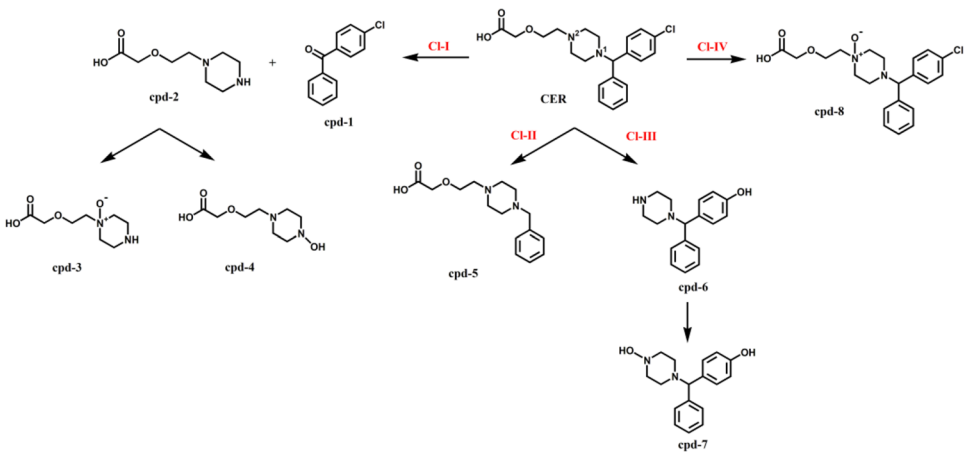

Fig. 10 Possible degradation pathways of CER oxidized by NaClO

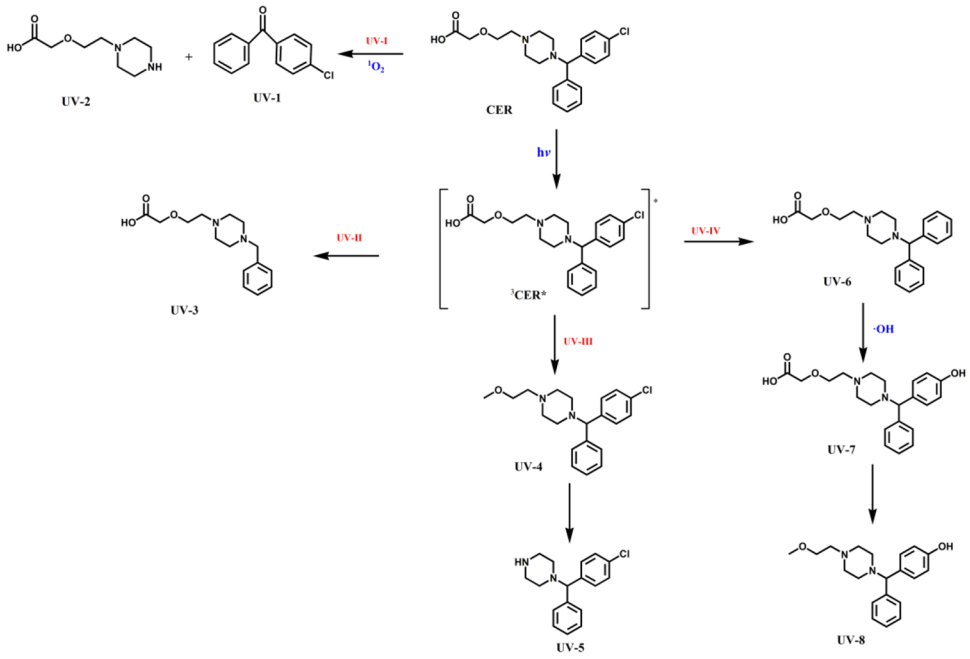

Fig. 11 Possible degradation pathways of CER photolysis

For cpd-5 and UV-3, the third group of the same products, the para-position of the chlorine substituent was active and easily oxidized (Pathway Cl-II), which led to the breaking of the carbon–carbon single bond and the removal of the chlorine-containing benzene ring to form cpd-5 (Li et al. 2019). In the photolysis process (Pathway UV-II), CER was transformed into a triple excited state (^{3}CER*) after absorbing photons. ^{3}CER* formed UV-3 through the fracture of chlorine-containing benzene rings and the hydrogen extraction reaction process.

The remaining products of chlorine oxidation and photolysis were different. For the chlorine oxidation pathway Cl-I, cpd-2, containing a secondary amine and a tertiary amine group, could be further oxidized on the nitrogen atom, which formed the corresponding N-oxide on the tertiary amine or the corresponding hydroxylamine on the secondary amine, namely cpd-3 and cpd-4.

Chlorine oxidation pathway Cl-III: The N_2-amine in the CER molecule was dealkylated, and then the chlorine atom was replaced by the hydroxyl group to form cpd-6. The secondary amine was oxidized to form the corresponding hydroxylamine and subsequently to form cpd-7.

Chlorine oxidation pathway Cl-IV: The composition of NaClO in aqueous solution is complex, and the form of hypochlorous acid could decompose and generate new atomic oxygen [O], which has strong oxidizing properties (Sun et al. 2019). In addition, many studies have shown that tertiary amines can react with oxidants to form nitrogen oxides, so the tertiary amines in the CER molecule may be attacked by [O]. Similar to FEX, nitrogen may be the main attack site of oxidizing agents, and we speculated that Cl-IV was the main pathway. The CER molecule contained two tertiary amines, and the oxidant could attack the tertiary amine to form nitrogen oxides. However, it was not clear which tertiary amine was attacked first based on the mass spectrum information. Borowska et al. (2016) reported that N_2-amine was more active than N_1-amine, so the N_2-oxide of CER was easier to form than the N_1-oxide, forming cpd-8. It is worth noting that chlorine oxidation of amine-containing compounds had a unique reaction. Chlorine attacks the N in the compounds to form chlorinated amines. CER contained tertiary amines, but in the process of product identification, the expected product was not found; because of reaction with thiosulfate, chlorinated amines could be converted back into the parent compound (Pinkston and Sedlak 2004).

Photolysis pathways UV-III and UV-IV: ^{3}CER* cracked and removed carboxyl groups to form UV-4, and subsequent dealkylation resulted in the formation of UV-5. Under ultraviolet light irradiation, dechlorination may be the first reaction to occur (Zheng and Ye 2001). CER absorbed photons and then dechlorinated to form UV-6. Chlorine was an electron-withdrawing group; after being removed, the electron cloud density on the benzene ring increased, and it was easily attacked by HO· radicals (Li and Ma 2006). Hydroxylation occurred to form UV-7, and UV-8 was formed by decarboxylation of UV-7.

Limitations and future works

As an emerging advanced oxidation technology, UV-NaClO requires further research on its reaction mechanism and influencing factors, and research on the degradation pathway of drugs also needs to be improved. To accurately assess

the main degradation pathways of drugs in the oxidation process of UV alone and NaClO alone, we need to use more analytical methods to verify the degradation intermediates and quantify them for further analysis. We found that the acute toxicity of the intermediate product has increased, which will limit the application of disinfection methods to a certain extent. The choice of indicator organisms also has a certain influence on the effect of toxicity. In addition, we will explore the effects of the complicated components in the actual water body on the oxidative degradation of drugs to provide more valid and reliable information for the water treatment process.

Conclusions

This study comprehensively compared the degradation efficiencies of antihistamine drugs (loratadine, cetirizine, fexofenadine) by three different oxidation methods. The results showed:

(1) In the NaClO system, the degradation efficiencies were affected by the existing forms of the drugs and free chlorine, which changed with solution pH. As the pH increased, the degradation efficiencies of LOR decreased from 11% to 3%, while FEX increased from 11% to 92%. CER had better degradation efficiencies under strong acid and strong alkaline conditions, which were greater than 85%. Due to the photosensitivity of the three drugs, their degradation efficiencies were more than 75% with UV irradiation within 150 s at a pH of 7, which were far more than those of NaClO oxidation. Among the three oxidation methods, UV-NaClO had the best effect on drug degradation under most conditions.

(2) In the process of photolysis, $^1O_2$ played an important role. For FEX and CER, the contribution rates of $^1O_2$ reached 70%; for LOR, the contributions of $^3ANT^*$ and $^1O_2$ were very close, and the rates were 49.7% and 46.2%, respectively.

(3) Aqueous matrices had different influence on the oxidation efficienciesof the drugs. The influence of aqueous matrices on the UV system was more significant than that on the NaClO system. The aqueous matrices affected not only the photolysis process through the light-shielding effect but also the removal and excitation of active species.

(4) The drugs could not be completely mineralized, and the toxicities of the degradation intermediates were even higher than those of the parent drugs. Several degradation pathways were first proposed by the identification of degradation intermediates.

Supplementary Information The online version contains supplementary material available at https://doi.org/10.1007/s11356-022-18760-8.

Acknowledgements This work was supported by the National Natural Science Foundation of China (Grant number 41877466) and Natural Science Foundation of Guangdong Province (Grant number 2019A1515011037).

Author contributions All authors contributed to the study conception and design. Material preparation and experimental operation was performed by Anchen Liu, Wenqi Guan, Ningyi Hu, and Sichun Zheng. Data collection and analysis was performed by Anchen Liu and Wenting Lin. Products identification was performed by Senwen Ping. Conceptualization, writing—reviewing and editing, supervision was performed by Yuan Ren. The first draft of the manuscript was written by Anchen Liu and all authors commented on previous versions of the manuscript. All authors read and approved the final manuscript.

Funding All sources of financial support had been disclosed in the Acknowledgments.

Availability of data and materials All data generated or analyzed during this study are included in this published article [and its supplementary information files].

Declarations

This paper is our original work and we have not already published in another journal a paper describing essentially the same material, nor is this paper currently being considered for publication in another journal.
Authorship of the paper included all those who have made significant contributions to the work and they are listed as co-authors.
All co-authors have approved the final version of the paper and have agreed to its submission for publication.
All authors accepted these principles as mentioned above.

Competing interests The authors have no relevant financial or non-financial interests to disclose.

Ethics approval and consent to participate Not applicable.

Consent for publication Not applicable.

References

Abounassif MA, El-Obeid HA, Gadkariem EA (2005) Stability studies on some benzocycloheptane antihistaminic agents. J Pharm Biomed Anal 36(5):1011–1018. https://doi.org/10.1016/j.jpba.2004.09.019

Aghdam E, Xiang YY, Sun JL, Shang C, Yang X, Fang JY (2017) DBP formation from degradation of DEET and ibuprofen by UV/chlorine process and subsequent post-chlorination. J Environ Sci 58:146–154. https://doi.org/10.1016/j.jes.2017.06.014

Armaković S, Armaković SJ, Abramović BF (2016) Theoretical investigation of loratadine reactivity in order to understand its degradation properties: DFT and MD study. J Mol Model 22(10). https://doi.org/10.1007/s00894-016-3101-2

Bahlmann A, Carvalho JJ, Weller MG, Panne U, Schneider RJ (2012) Immunoassays as high-throughput tools: Monitoring spatial and temporal variations of carbamazepine, caffeine and cetirizine in surface and wastewaters. Chemosphere 89(11):1278–1286. https://doi.org/10.1016/j.chemosphere.2012.05.020

Bergheim M, Gminski R, Spangenberg B, Dębiak M, Bürkle A, Mersch-Sundermann V, Kümmerer K, Gieré R (2014) Recalcitrant pharmaceuticals in the aquatic environment: a comparative screening study of their occurrence, formation of phototransformation products and their in vitro toxicity. Environ Chem 11(4):431. https://doi.org/10.1071/EN13218

Bilski P, Martinez LJ, Koker EB, Chignell CF (1996) Photosensitization by Norfloxacin is a Function of pH. Photochem Photobiol 64(3):496–500. https://doi.org/10.1111/j.1751-1097.1996.tb03096.x

Bodhipaksha LC, Sharpless CM, Chin YP, MacKay AA (2017) Role of effluent organic matter in the photochemical degradation of compounds of wastewater origin. Water Res 110:170. https://doi.org/10.1016/j.watres.2016.12.016

Boreen AL, Arnold WA, McNeill K (2003) Photodegradation of pharmaceuticals in the aquatic environment: A review. Aquat Sci 65(4):320–341. https://doi.org/10.1007/s00027-003-0672-7

Borowska E, Bourgin M, Hollender J, Kienle C, McArdell CS, Gunten UV (2016) Oxidation of cetirizine, fexofenadine and hydrochlorothiazide during ozonation: Kinetics and transformation products. Water Res 94:350–362. https://doi.org/10.1016/j.watres.2016.02.020

Breier AR, Nudelman NS, Steppe M, Schapoval EES (2008) Isolation and structure elucidation of photodegradation products of fexofenadine. J Pharm Biomed Anal 46(2):250–257. https://doi.org/10.1016/j.jpba.2007.09.017

Cai MQ, Zhang LQ, Qi F, Feng L (2013) Influencing factors and degradation products of antipyrine chlorination in water with free chlorine. J Environ Sci 25(1):77–84. https://doi.org/10.1016/S1001-0742(12)60003-5

Cronin MTD, Manga N, Seward JR, Sinks GD, Schultz TW (2001) Parametrization of Electrophilicity for the Prediction of the Toxicity of Aromatic Compounds. Chem Res Toxicol 14(11):1498–1505. https://doi.org/10.1021/tx015502k

Derbalah A, Sunday M, Kato R, Takeda K, Sakugawa H (2020) Photoformation of reactive oxygen species and their potential to degrade highly toxic carbaryl and methomyl in river water. Chemosphere 244:125464. https://doi.org/10.1016/j.chemosphere.2019.125464

Dodd MC, Shah AD, Gunten UV, Huang CH (2005) Interactions of Fluoroquinolone Antibacterial Agents with Aqueous Chlorine: Reaction Kinetics, Mechanisms, and Transformation Pathways. Environ Sci Technol 39(18):7065–7076. https://doi.org/10.1021/es050054e

Dong HY, Qiang ZM, Hu J, Qu JH (2017) Degradation of chloramphenicol by UV/chlorine treatment: Kinetics, mechanism and enhanced formation of halonitromethanes. Water Res 121:178–185. https://doi.org/10.1016/j.watres.2017.05.030

Dyakonov T, Muir A, Nasri H, Toops D, Fatmi A (2010) Isolation and Characterization of Cetirizine Degradation Product: Mechanism of Cetirizine Oxidation. Pharm Res 27(7):1318–1324. https://doi.org/10.1007/s11095-010-0114-x

Editorial Department Of Annual Report (2015) Chemical pharmaceuticals division in 2013 China medical statistics annual report. Ministry of Industry and Information Technology of China, Beijing, p 137

Editorial Department Of Annual Report (2016) Chemical pharmaceuticals division in 2014 China medical statistics annual report. Ministry of Industry and Information Technology of China, Beijing, p 137

Editorial Department Of Annual Report (2017) Chemical pharmaceuticals division in 2015 China medical statistics annual report. Ministry of Industry and Information Technology of China, Beijing, p 135

Fang JY, Fu Y, Shang C (2014) The Roles of Reactive Species in Micropollutant Degradation in the UV/Free Chlorine System. Environ Sci Technol 48(3):1859–1868. https://doi.org/10.1021/es4036094

Faria CV, Ricci BC, Silva AFR, Amaral MCS, Fonseca FV (2020) Removal of micropollutants in domestic wastewater by expanded granular sludge bed membrane bioreactor. Process Saf Environ 136:223–233. https://doi.org/10.1016/j.psep.2020.01.033

Gadipelly CR, Rathod VK, Marathe KV (2016) Persulfate assisted photo-catalytic abatement of cetirizine hydrochloride from aqueous waste: Biodegradability and toxicity analysis. J Mol Catal A Chem 414:116–121. https://doi.org/10.1016/j.molcata.2015.12.021

Gallard H, Gunten VU (2002) Chlorination of Phenols: Kinetics and Formation of Chloroform. Environ Sci Technol 36(5):884–890. https://doi.org/10.1021/es010076a

Gligorovski S, Strekowski R, Barbati S, Vione D (2015) Environmental Implications of Hydroxyl Radicals (•OH). Chem Rev 115(24):13051–13092. https://doi.org/10.1021/cr500310b

Golovko O, Kumar V, Fedorova G, Randak T, Grabic R (2014) Seasonal changes in antibiotics, antidepressants/psychiatric drugs, antihistamines and lipid regulators in a wastewater treatment plant. Chemosphere 111:418–426. https://doi.org/10.1016/j.chemosphere.2014.03.132

Golovko O, Anton LdB, Cascone C, Ahrens L, Lavonen E, Köhler SJ (2020) Sorption Characteristics and Removal Efficiency of Organic Micropollutants in Drinking Water Using Granular Activated Carbon (GAC) in Pilot-Scale and Full-Scale Tests. Water 12(7):2053. https://doi.org/10.3390/w12072053

Gumieniczek A, Berecka-Rycerz A, Pietraś R, Kozak I, Lejwoda K, Kozyra P (2019) Comparative Study of Chemical Stability of Two H1 Antihistaminic Drugs, Terfenadine and Its In Vivo Metabolite Fexofenadine, Using LC-UV Methods. J Anal Methods Chem 2019:1–10. https://doi.org/10.1155/2019/5790404

Gunjal RP, Raju G, Babu A, Mallikarjun N, Shastri N (2011) Srinivas R (2011) HPLC and LC-MS studies on stress degradation behavior of levocetirizine and development of a validated specific stability-indicating method. J Liq Chromatogr Relat Technol 34(12):955–965. https://doi.org/10.1080/10826076.2011.564704

Henning N, Falas P, Castronovo S, Jewell KS, Bester K, Ternes TA, Wick A (2019) Biological transformation of fexofenadine and sitagliptin by carrier-attached biomass and suspended sludge from a hybrid moving bed biofilm reactor. Water Res 167:115034. https://doi.org/10.1016/j.watres.2019.115034

Hu JY, Xie GH, Xiang ZGZ (2002) Aqueous chlorination pathways of 4-nonylphenol. Environ Chem 21(3):253–257. (in Chinese). https://doi.org/10.3321/j.issn:0254-6108.2002.03.009

Iesce MR, Lavorgna M, Russo C, Piscitelli C, Passananti M, Temussi F, DellaGreca M, Cermola F, Isidori M (2019) Ecotoxic effects of loratadine and its metabolic and light-induced derivatives. Ecotoxicol Environ Saf 170:664–672. https://doi.org/10.1016/j.ecoenv.2018.11.116

Ji YF, Zeng C, Ferronato C, Chovelon JM, Yang X (2012a) Nitrate-induced photodegradation of atenolol in aqueous solution: Kinetics, toxicity and degradation pathways. Chemosphere 88(5):6. https://doi.org/10.1016/j.chemosphere.2012.03.050

Ji YF, Zeng C, Lei Z, Yang X, Gao SX (2012) Photodegradation of atenolol under simulated solar irradiation. Acta Sci Circumstantiae 32(06):1357-1363.44–649. (in Chinese). https://doi.org/10.13671/j.hjkxxb.2012.06.021

Ji XL, Lv WY, Li FH, Chen P, Li RB, Fan SN, Yao K, Zhang XD, Liu GG (2016) Degradation of naproxen in water by sodium hypochlorite. Chin J Environ Eng 10(01):243–247. (in Chinese)

Jiang C, Lian JF, Sun L, Zhu YC, Sha HC (2018) Review on UV/chlorine advanced oxidation process. Mod Chem Ind 38(11):29–33. (in Chinese). https://doi.org/10.16606/j.cnki.issn0253-4320.2018.11.007

Jonsson M, Fick J, Klaminder J, Brodin T (2014) Antihistamines and aquatic insects: Bioconcentration and impacts on behavior in damselfly larvae (Zygoptera). Sci Total Environ 472:108–111. https://doi.org/10.1016/j.scitotenv.2013.10.104

Kosonen J, Kronberg L (2009) The occurrence of antihistamines in sewage waters and in recipient rivers. Environ Sci Pollut Res 16(5):555–564. https://doi.org/10.1007/s11356-009-0144-2

Kostich MS, Batt AL, Lazorchak JM (2014) Concentrations of prioritized pharmaceuticals in effluents from 50 large wastewater treatment plants in the US and implications for risk estimation. Environ Pollut 184:354–359. https://doi.org/10.1016/j.envpol.2013.09.013

Kristofco LA, Brooks BW (2017) Global scanning of antihistamines in the environment: Analysis of occurrence and hazards in aquatic systems. Sci Total Environ 592:477–487. https://doi.org/10.1016/j.scitotenv.2017.03.120

Larson RA, Rockwell AL (1979) Chloroform and chlorophenol production by decarboxylation of natural acids during aqueous chlorination. Environ Sci Technol 13(3):325–329. https://doi.org/10.1021/es60151a014

Li LXY, Ma XJ (2006) Characteristics of Hydroxide Radical and its Reaction Mechanism in Photochemistry Oxidation Process. Technol Dev Chem Ind 35(8):27–29. (in Chinese). https://doi.org/10.3969/j.issn.1671-9905.2006.08.010

Li QG, Li XY, Mao S (2019) Quantitative Analysis and Graphical Visualization Interpretation of Mono-substituted Benzene Ring Localization Effect. Univ Chem 34(01):108–115. (in Chinese). https://doi.org/10.3866/PKU.DXHX201805042

Li P, Ge P, Ping SW, Lin WT, Zhang XH, Wei CH, Ren Y (2021) Photodegradation mechanism and influencing factors of asthma drug salmeterol under UV irradiation. J Photochem Photobiol A 404:112944. https://doi.org/10.1016/j.jphotochem.2020.112944

Lin WT, Zhang XH, Li P, Tan YZ, Ren Y (2020) Ultraviolet photolysis of metformin: mechanisms of environmental factors, identification of intermediates, and density functional theory calculations. Environ Sci Pollut Res 27(14):17043–17053. https://doi.org/10.1007/s11356-020-08255-9

Liu Q, Wei DB, Chen ZB, Du YG (2012) A review on transformation behaviors of PPCPs in chlorination process. Environ Chem 31(03):278–286. (in Chinese)

Lv DM (2019) Application of multi-barrier disinfection strategy and UV disinfection technology in drinking water. Water Purif Technol 38(01):1–6. (in Chinese). https://doi.org/10.15890/j.cnki.jsjs.2019.01.001

Nödler K, Voutsa D, Licha T (2014) Polar organic micropollutants in the coastal environment of different marine systems. Mar Pollut Bull 85(1):50–59. https://doi.org/10.1016/j.marpolbul.2014.06.024

Ozaki N, Tanaka T, Kindaichi T, Ohashi A (2021) Photodegradation of fragrance materials and triclosan in water: Direct photolysis and photosensitized degradation. Environ Technol Innov 23:101766. https://doi.org/10.1016/j.eti.2021.101766

Pan ZH, Zhu YJ, Wei M, Zhang YY, Yu KF (2021) Interactions of fluoroquinolone antibiotics with sodium hypochlorite in bromide-containing synthetic water: Reaction kinetics and transformation pathways. J Environ Sci 102:170–184. https://doi.org/10.1016/j.jes.2020.09.013

Ping SW, Lin WT, Liu AC, Gao ZH, Lin H, Ren Y (2021) Ultraviolet photolysis of four typical cardiovascular drugs: mechanisms, influencing factors, degradation pathways, and toxicity trends. Environ Sci Pollut Res:1-13.https://doi.org/10.1007/s11356-021-15000-3

Pinkston KE, Sedlak DL (2004) Transformation of Aromatic Ether-and Amine-Containing Pharmaceuticals during Chlorine Disinfection. Environ Sci Technol 38(14):4019–4025. https://doi.org/10.1021/es035368l

Soufan M, Deborde M, Delmont A, Legube B (2013) Aqueous chlorination of carbamazepine: Kinetic study and transformation product identification. Water Res 47(14):5076–5087. https://doi.org/10.1016/j.watres.2013.05.047

Sun YQ, Song ZM, Situ F (2019) Application of sodium hypochlorite disinfection in waterworks. Ind Water Wastewater 50(1):5–7. (in Chinese). https://doi.org/10.3969/j.issn.1009-2455.2019.01.002

Tarozzi A, Andrisano V, Fiori J, Cavrini V, Forti GC, Hrelia P (2003) Photomutagenic properties of terfenadine as revealed by a stepwise photostability, phototoxicity and photomutagenicity testing approach. Photochem Photobiol 77(4):356–361. https://doi.org/10.1562/0031-8655(2003)077%3c0356:PPOTAR%3e2.0.CO;2

Vione D, Feitosa-Felizzola J, Minero C, Chiron S (2009) Phototransformation of selected human-used macrolides in surface water: Kinetics, model predictions and degradation pathways. Water Res 43(7):1959–1967. https://doi.org/10.1016/j.watres.2009.01.027

Wang YF, Roddick FA, Fan LH (2017) Direct and indirect photolysis of seven micropollutants in secondary effluent from a wastewater lagoon. Chemosphere. https://doi.org/10.1016/j.chemosphere.2017.06.122

Wu JH (2012) Types and application strategy of the second-generation antihistamines. Pharm Care Res 12(05):321-325. (in Chinese). https://doi.org/10.5428/pcar20120501

Wu QY, Li Y, Wang WL, Wang T, Hu HY (2016) Removal of Cl Reactive Red 2 by low pressure UV/chlorine advanced oxidation. J Environ Sci 41:227–234. https://doi.org/10.1016/j.jes.2015.06.013

Wu YT, Zhu S, Zhang WQ, Bu LJ, Zhou SQ (2019) Comparison of diatrizoate degradation by UV/chlorine and UV/chloramine processes: Kinetic mechanisms and iodinated disinfection byproducts formation. Chem Eng J 375:121972. https://doi.org/10.1016/j.cej.2019.121972

Xu YJ, Lin JY (2006) Identification of the metabolite of cetirizine hydrochloride by HPLC-ESi/ MS^n. Chin J Hosp Pharm 08:952–954. (in Chinese). https://doi.org/10.3321/j.issn:1001-5213.2006.08.015

Yan JN, Zhang XH, Ren Y (2017) Kinetic and Influencing Factors of Diclofenac Oxidation in Water by Sodium Hypochlorite. Technol Water Treat 43(09):56–61. (in Chinese). https://doi.org/10.16796/j.cnki.1000-3770.2017.09.012

Yang YJ, Shi JC, Yang Y, Yin J, Zhang J, Shao B (2019) Transformation of sulfamethazine during the chlorination disinfection process: Transformation, kinetics, and toxicology assessment. J Environ Sci 76:48–56. https://doi.org/10.1016/j.jes.2018.03.024

Yassine M, Rifai A, Doumyati S, Trivella A, Mazellier P, Budzinski H, Al Iskandarani M (2017) Oxidation of danofloxacin by free chlorine-kinetic study, structural identification of by-products by LC-MS/MS and potential toxicity of by-products using in silico test. Environ Sci Pollut Res 24(9):7982–7993. https://doi.org/10.1007/s11356-017-8409-7

Yu WW, Zhao ZK (2019) Catalyst-Free Selective Oxidation of Diverse Olefins to Carbonyls in High Yield Enabled by Light under Mild Conditions. Org Lett 21(19):7726–7730. https://doi.org/10.1021/acs.orglett.9b02569

Zhang FZ, Wu CF, Hu Y, Wei CH (2014) Photochemical degradation of halogenated organic contaminants. Prog Chem 26(06):1079–1098. https://doi.org/10.7536/PC131134

Zhang CS, Ni Z, Ye JC, Wu DS, Liu M (2021) Determination of 15 antihistamine agents illegally added into herbal medicines and dietary supplements by UPLC-MS/MS. Cent South Pharm 19(05):954–957. (in Chinese). https://doi.org/10.7539/j.issn.1672-2981.2021.05.029

Zheng HH, Ye CM (2001) Identification of UV Photoproducts and Hydrolysis Products of Butachlor by Mass Spectrometry. Environ

Sci Technol 35(14):2889–2895. https://doi.org/10.1021/es0016811

Zhou HD, Ying TQ, Wang XL, Liu JB (2016) Occurrence and preliminarily environmental risk assessment of selected pharmaceuticals in the urban rivers, China. Sci Rep 6(1). https://doi.org/10.1038/srep34928

Zhuang HC, Li X, Xiang F (2010) Research progress on the pharmacological effects and mechanism of desloratadine. Cent South Pharm 8(01):48–51. (in Chinese)

Authors and Affiliations

Anchen Liu[1] · Wenting Lin[1] · Senwen Ping[1] · Wenqi Guan[1] · Ningyi Hu[1] · Sichun Zheng[1] · Yuan Ren[1,2,3]

[1] School of Environment and Energy, South China University of Technology, Higher Education Mega Center, Panyu District, Guangzhou 510006, People's Republic of China

[2] The Key Laboratory of Pollution Control and Ecosystem Restoration in Industry Clusters, Ministry of Education, Guangzhou 510006, People's Republic of China

[3] The Key Laboratory of Environmental Protection and Eco-Remediation of Guangdong Regular Higher Education Institutions, Guangzhou 510006, People's Republic of China